Biochem. J. (2013) **449**, 673–681 (Printed in Great Britain) doi:10.1042/BJ20120952

Rfa2 is specifically dephosphorylated by Pph3 in *Candida albicans*

Haitao WANG*†[1], Jiaxin GAO*[1], Ada Hang-Heng WONG‡, Kangdi HU*, Wanjie LI*, Yue WANG†[2] and Jianli SANG*[2]

*Key Laboratory of Cell Proliferation and Regulation Biology, Ministry of Education, College of Life Sciences, Beijing Normal University, Beijing 100875, People's Republic of China, †Institute of Molecular and Cell Biology, Agency for Science, Technology and Research (A*STAR), Singapore 138673, and ‡Protein Science Laboratory, School of Life Sciences, Tsinghua University, Beijing 100084, People's Republic of China

Rfa2 is a ssDNA (single-stranded DNA)-binding protein that plays an important role in DNA replication, recombination and repair. Rfa2 is regulated by phosphorylation, which alters its protein–protein interaction and protein–DNA interaction. In the present study, we found that the Pph3–Psy2 phosphatase complex is responsible for Rfa2 dephosphorylation both during normal G_1-phase and under DNA replication stress in *Candida albicans*. Phosphorylated Rfa2 extracted from *pph3Δ* or *psy2Δ* G_1 cells exhibited diminished binding affinity to dsDNA (double-stranded DNA) but not to ssDNA. We also discovered that Cdc28 (cell division cycle 28) and Mec1 are responsible for Rfa2 phosphorylation in G_1-phase and under DNA replication stress respectively. Moreover, MS revealed that the domain of Rfa2 that was phosphorylated in G_1-phase differed from that phosphorylated under the stress conditions. The results of the present study imply that differential phosphorylation plays a crucial role in RPA (replication protein A) regulation.

Key words: dephosphorylation, DNA replication, phosphatase, protein–DNA interaction, replication protein A (RPA).

INTRODUCTION

RPA (replication protein A) is a heterotrimeric complex that functions in DNA replication, repair and recombination pathways in eukaryotes [1–4]. It consists of three subunits of 70, 32 and 14 kDa respectively, namely RPA1 or RPA70, RPA2 or RPA32, and RPA3 or RPA14 (known as Rfa1, Rfa2 and Rfa3 respectively in *Saccharomyces cerevisiae*) [1,3–6]. RPA1 consists of four OB (oligonucleotide-binding) fold DBDs (DNA-binding domains), named DBD-F, DBD-A, DBD-B and DBD-C [3,4]. The N-terminal DBD-F and DBD-A domains of RPA1 have been implicated in the recruitment of other factors during DNA replication, repair or recombination [7–9], whereas the C-terminal DBD-C domain is essential for RPA trimerization [3,4,10,11]. RPA2 contains a flexible NTD (N-terminal domain) that is highly phosphorylated, a DBD, DBD-D, and a CTD (C-terminal domain) that mediates protein–protein interactions [3,12–15]. RPA3 contains a single DBD, DBD-E, which interacts with DBD-D of RPA2 and DBD-C of RPA1 to form a stable RPA trimer.

The RPA heterotrimeric complex has a high affinity for ssDNA (single-stranded DNA) in a 5′→3′ polar manner [16–22]. It binds to ssDNA ranging from 8 to 30 nt [11], seemingly with low sequence specificity. DBD-A and DBD-B of RPA1 have the highest DNA-binding affinities [3,21]. Various binding modes requiring different DBDs in the trimeric RPA have been presented [3,22–25]. However, distinct from RPA1, DBD-D of RPA2 also interacts with dsDNA (double-stranded DNA) and plays an important role in DNA priming during early DNA replication [4]. Moreover, Dickson et al. [26] showed that an RPA2 DBD-D mutant with compromised DNA-binding activity has little effect on cell viability.

RPA is phosphorylated in a cell-cycle-dependent manner [27–29]. RPA2 is preferentially phosphorylated, especially at its NTD [3–5]. RPA2 is phosphorylated at Ser^{23} in S-phase, and simultaneously at Ser^{23} and Ser^{29} in M-phase [30]. Phosphorylated RPA2 extracted from mitotic HeLa cells resulted in lower dsDNA-binding affinity, but had no effect on ssDNA binding [31]. RPA2 phosphorylation also abolished its binding to DNA replication and repair proteins such as ATM (ataxia telangiectasia mutated), DNA-PK (DNA-dependent protein kinase) and DNA polymerase α [31]. Furthermore, phosphorylated RPA also showed weaker RPA1–RPA2 interactions [32]. In addition, DNA damage is another key factor triggering RPA hyperphosphorylation, which is, however, distinct from the cell-cycle-dependent phosphorylation. Ionizing radiation led to RPA2 localization to DNA damage loci and RPA2 hyperphosphoryation which involves ATM and DNA-PK [30]. Bleomycin-treated cells undergoing mitosis led to RPA2 phosphorylation at Ser^4/Ser^8 and Thr^{21} which are primed by phosphorylation at Ser^{23} and Ser^{29} [33,34]. Ser^4 and Ser^8 was demonstrated to be phosphorylated during DSB (double-strand break) of DNA leading to stalled DNA replication [13,35–37]. Furthermore, RPA2 was shown to be phosphorylated at Ser^{11}, Ser^{12}, Ser^{13}, Thr^{21}, Ser^{23}, Ser^{29} and Ser^{33} by ATM and DNA-PK *in vitro*, many of which coincide with those phosphorylated *in vivo* in response to DNA damage [13,36,38–41]. Hence, phosphorylation plays a pivotal role in regulating RPA activity [39,42]. Currently, studies of the phosphatases involved in the phosphoregulation of RPA2 are limited. The PP2A-like phosphatases PP2AC and PP4C have been implicated in dephosphorylating RPA2 in the DNA-damage response [43,44]. However, the phosphatase(s) responsible for RPA2 dephosphorylation during G_1-phase remains elusive [43,44].

In the present study, we found that the Pph3–Psy2 phosphatase complex is responsible for Rfa2 dephosphorylation both during normal G_1-phase and under DNA replication stress in *Candida*

Abbreviations used: AP, alkaline phosphatase; ATM, ataxia telangiectasia mutated; Cdc, cell division cycle; CDK, cyclin-dependent kinase; co-IP, co-immunoprecipitation; CTD, C-terminal domain; DBD, DNA-binding domain; DNA-PK, DNA-dependent protein kinase; DSB, double-strand break; dsDNA, double-stranded DNA; EMSA, electrophoretic mobility-shift assay; FL, full-length; GFP, green fluorescent protein; GMM, glucose minimal medium; HF, hyphal form; HU, hydroxyurea; λPPase, lambda phosphatase; NTD, N-terminal domain; PI3K, phosphoinositide 3-kinase; RPA, replication protein A; ssDNA, single-stranded DNA; TBST, Tris-buffered saline containing 0.1 % Tween 20; TGE, Tris-glycine-EDTA; UTR, untranslated region; WT, wild-type; YF, yeast form.

[1] These authors contributed equally to this work.

[2] Correspondence may be addressed to either of these authors (email jlsang@bnu.edu.cn or mcbwangy@imcb.a-star.edu.sg).

albicans. Moreover, the results of the present study showed that the domain of Rfa2 phosphorylated during G_1-phase differed from that phosphorylated in response to DNA replication stress, indicating that differential phosphorylation plays a crucial role in RPA regulation in *C. albicans*.

MATERIALS AND METHODS

Strains and culture conditions

All *C. albicans* strains used in the present study are listed in Supplementary Table S1 (at http://www.biochemj.org/bj/449/bj4490673add.htm). Except where noted, *C. albicans* were routinely grown at 30 °C in YPD medium (1 % yeast extract, 2 % peptone and 2 % glucose), in GMM (glucose minimal medium; 2 % glucose and 6.79 g/l yeast nitrogen base without amino acids) or in GMM supplemented with the required nutrients for auxotrophic mutants. Solid media contained 2 % agar.

Preparation of G_1 cells, induction of hyphal growth by serum and HU (hydroxyurea) treatment of cells

G_1 cells were obtained by growing yeast cultures at 30 °C for 72 h until >90 % of cells were found in G_1-phase under the microscope. Then the cells were released into fresh YPD medium as described previously [45].

For hyphal growth, bovine serum was added to *C. albicans* yeast cells in YPD medium to a final concentration of 20 % and the cells were incubated at 37 °C for 4 h before harvesting the cells for analysis.

To cause DNA replication stress, HU was added to *C. albicans* cultures in YPD medium to a final concentration of 20 mM, and the cells were incubated at 30 °C for a specified time. Recovery from the DNA replication stress was achieved by shifting the cells to fresh HU-free YPD medium and incubation at 30 °C for 4–6 h before harvesting cells for analysis.

Construction of *C. albicans* mutant strains

C. albicans homologues of *S. cerevisiae* genes were identified by sequence alignment in the *C. albicans* genome database (http://www.candidagenome.org). *C. albicans* deletion mutants were constructed by sequentially deleting the two copies of the target gene with two deletion cassettes from the WT (wild-type) strain of BWP17. The deletion cassettes were constructed by flanking a selectable marker gene (*ARG4* or *HIS1*) with the AB and CD DNA fragments (~400 bp each), which correspond to the 5′ and 3′ UTRs (untranslated regions) of the target gene respectively [45]. Homozygous deletion mutants were verified by PCR.

For rescue experiments, the entire ORF (open reading frame) of the target gene, together with its promoter (~1000 bp), was cloned into the CIp10-based *URA3*-marked plasmid at KpnI and ClaI sites, followed by the *GAL4* 3′ UTR. The construct was linearized with StuI, whose site exists in the RP10 sequence of the plasmid CIp10, and finally introduced into the gene deletion strains [45].

Construction of *C. albicans* strains expressing C-terminal Myc-tagged Rfa2 or truncated Rfa2 fragments was carried out as described previously [46]. C-terminal GFP (green fluorescent protein)-tagged Rfa2 was constructed in the WT *C. albicans* strain as described above. For affinity purification of Rfa2, C-terminal His-tagged full-length Rfa2 was constructed in the WT strain, and *pph3Δ* and *psy2Δ* mutants in a similar fashion.

Protein extraction, Western blotting, protein dephosphorylation and co-IP (co-immunoprecipitation)

To extract proteins, cells were harvested by centrifugation (4000 ***g*** for 5 min at 4 °C), and ~100 mg of cell pellet was resuspended in 300 μl of ice-cold RIPA buffer [50 mM Tris/HCl (pH 7.4), 150 mM NaCl, 1 % Nonidet P40, 0.5 % sodium deoxycholate and 0.1 % SDS]. After adding an equal volume of acid-washed glass beads (Sigma–Aldrich), the cells were lysed by four rounds of 45 s of beating at 5000 rev./min in a MicroSmash MS-100 bead beater (Tomy Medico) with 2 min of cooling on ice between rounds. The supernatant was collected after centrifugation of the cell lysate at 16000 ***g*** for 20 min at 4 °C. The protein concentration of the lysate was determined using the bicinchoninic acid protein assay (Galen).

For Western blot analysis, 30 μg of total protein was separated by SDS/PAGE (10 % or 12 % gels) and transferred on to a PVDF membrane (Millipore). The membrane was immersed in TBST [TBS (Tris-buffered saline, pH 7.4) containing 0.1 % Tween 20] and 5 % non-fat dried skimmed milk for 1 h at room temperature (25 °C), followed by primary antibody and secondary antibody conjugated to hydrogen peroxidase or AP (alkaline phosphatase) consecutively for 1 h each, both in TBST containing 1 % non-fat dried skimmed milk. The target protein was visualized by using the ECL (enhanced chemiluminescence) system or AP system. Anti-Myc and anti-Cdc28 (cell division cycle 28) (PSTAIRE) antibodies were purchased from Santa Cruz Biotechnology.

Protein dephosphorylation was carried out as described previously [45]. λPPase (lambda phosphatase) was purchased from New England BioLabs (catalogue number P07535).

A co-IP assay was performed by using an anti-Myc antibody to first pull down the Myc-tagged protein. Then co-immunoprecipitated proteins were detected by Western blot analysis with appropriate antibodies as described above.

Protein purification and EMSA (electrophoretic mobility-shift assay)

WT *C. albicans* and *pph3Δ* and *psy2Δ* mutant cells expressing C-terminal His-tagged full-length Rfa2 were grown in YPD medium at 30 °C for 3 days. Cells were harvested, lysed by cell disruption (Avestin) and centrifuged at 20000 ***g*** at 4 °C for 30 min. The supernatant was purified on gravity-flow Ni-NTA (Ni^{2+}-nitrilotriacetate) columns (Qiagen) followed by anion-exchange chromatography (SourceQ, GE Healthcare) on an Äkta purifier (GE Healthcare). Purified Rfa2 was concentrated by using centrifugal concentration tubes (Amicon, Millipore) until a final concentration of 0.8–1.0 mg/ml was reached.

An EMSA was performed with ssDNA of the sequence 5′-FITC-CCCCTCTCCTTCTTGGCCTCTTCCTTCCCC-3′ or dsDNA annealed from complementary strands of the sequences 5′-FITC-CCCCTCTCCTTCTTGGCCTCTTCCTTCCCC-3′ and 5′-GGG-GAAGGAAGAGGCCAAGAAGGAGAGGGG-3′ using standard protocols. Purified Rfa2 protein was mixed at ratios of 0, 3.12, 6.25 and 12.5 pmol to a constant amount of DNA of 400 pmol in a total reaction mixture of 20 μl and incubated at room temperature for 30 min. All reaction mixtures were loaded on to an 8 % TGE (Tris-glycine-EDTA) gel and run at 100 V at 4 °C for 1 h.

RESULTS

The Pph3–Psy2 complex is responsible for Rfa2 dephosphorylation during G_1-phase in *C. albicans*

Human RPA2 was found to be phosphorylated during mitosis and became hyperphosphorylated on DNA damage [3–5,31,33]. PP2A and PP4 were found to dephosphorylate RPA2 in humans

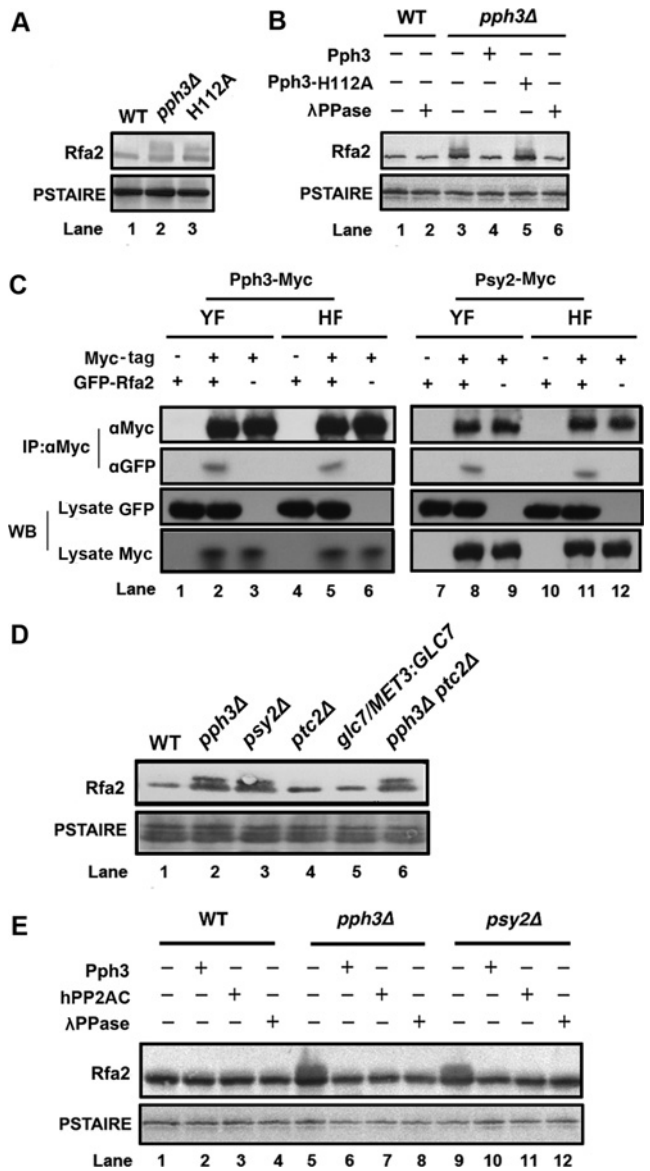

Figure 1 Pph3 is responsible for Rfa2 dephosphorylation during G_1-phase

(**A**) Western blot analysis of Rfa2 extracted from WT cells (HT1), *pph3Δ* cells (HT2) and *pph3Δ* cells expressing Pph3-H112A (HT29.1) in G_1-phase. G_1 cells were obtained by growing cells at 30 °C for 3 days until >90 % of the cells were in G_1-phase. (**B**) Western blot analysis of Rfa2 extracted from WT (HT1) and *pph3Δ* (HT2) G_1 cells. Pph3 affinity-purified from strain HT28, Pph3-H112A from HT29 or λPPase was used to treat immune-purified Rfa2 *in vitro*. (**C**) Co-IP analysis of Pph3 and Psy2 with Rfa2. *C. albicans* cells co-expressing Pph3–Myc and GFP–Rfa2 (HT26), and those co-expressing Psy2–Myc and GFP–Rfa2 (HT27) were grown as yeast (YF) or hyphae (HF). Cell lysates were prepared for co-IP. IP was performed using an anti-Myc antibody followed by Western blot (WB) analysis with an anti-Myc or anti-GFP antibody. (**D**) Western blot analysis of Rfa2 extracted from WT (HT1), *pph3Δ* (HT2), *psy2Δ* (HT3), *ptc2Δ* (HT4), *glc7/MET3:GLC7* (HT25) and *pph3Δ ptc2Δ* (HT5) cells during G_1 arrest. To shut down *GLC7* expression in HT25, the medium contained 0.5 mM each of methionine and cysteine. (**E**) Western blot analysis of Rfa2 extracted from WT (HT1), *pph3Δ* (HT2) and *psy2Δ* (HT3) G_1 cells. *C. albicans* Pph3, human PP2Ac or λPPase was used to treat purified Rfa2 *in vitro*.

after DNA damage [43,44]. However, the phosphatase responsible for RPA2 dephosphorylation during G_1-phase remained elusive. In the present study, we found that Pph3, the yeast homologue of PP4, dephosphorylates Rfa2 during G_1-phase *in vivo* and *in vitro* in *C. albicans*.

Western blot analysis of Rfa2 extracted from WT *C. albicans* G_1 cells exhibited a dephosphorylated form (Figure 1A). The deletion of *PPH3* or replacement of WT *PPH3* with the catalytic mutant allele *pph3-H112A* led to accumulation of phosphorylated Rfa2 in G_1 cells (Figure 1A). Furthermore, addition of antibody-purified Pph3 dephosphorylated Rfa2 in *pph3Δ* cell lysate (Supplementary Figure S1 at http://www.biochemj.org/bj/449/bj4490673add.htm), whereas addition of Pph3-H112A had no such effect (Figure 1B). Similarly, Rfa2 was dephosphorylated by the broad-specificity λPPase in the positive control (Figure 1B). Hence, the results strongly suggest that Pph3 dephosphorylates Rfa2 during G_1-phase in *C. albicans*.

In addition, we found that the regulatory subunit Psy2 (corresponding to human PP4R3) of Pph3 is involved in the interaction between Pph3 and Rfa2. Co-IP assays revealed that Rfa2 could be pulled down with Pph3 and Psy2 from both yeast and hyphal cells of *C. albicans* (Figure 1C). Whether both subunits directly interact with Rfa2 has not been investigated. Moreover, Rfa2 displayed a phosphorylated form in both the *pph3Δ* and the *psy2Δ* mutant (Figure 1D). This indicates that Psy2 is required for proper Rfa2 dephosphorylation during G_1-phase. Further investigations with deletion mutants of *ptc2* and *glc7*, the yeast homologues of PP2C and PP1, demonstrated that the *pph3Δ ptc2Δ* mutant resulted in Rfa2 phosphorylation during G_1-phase, whereas Rfa2 remained dephosphorylated in *ptc2Δ* and *glc7Δ* cells, similar to WT cells (Figure 1D). In addition, *in vitro* addition of Pph3, human PP2AC or λPPase dephosphorylated Rfa2 immunopurified from *pph3Δ* and *psy2Δ* cell lysates (Figure 1E). Hence, we concluded that Rfa2 is specifically dephosphorylated by the Pph3–Psy2 complex during G_1-phase in *C. albicans*.

Pph3 is responsible for Rfa2 dephosphorylation under DNA replication stress in *C. albicans*

In humans, DNA damage is known to lead to RPA2 hyperphosphorylation in a manner distinct from its phosphorylation during mitosis [3,4,33,34]. We next asked whether Pph3 is involved in Rfa2 dephosphorylation under DNA replication stress in *C. albicans*. Before addressing this question, we first wanted to check whether cell-cycle phases affect Rfa2 phosphorylation, as observed for RPA2 in human cells. We monitored Rfa2 phosphorylation at timed intervals after releasing G_1 yeast cells into both yeast and hyphal growth conditions. In WT YF (yeast form) cells, Rfa2 was not phosphorylated at time zero, but became phosphorylated between 60 and 120 min, and the phosphorylation started to diminish at 150 min (Figure 2A, top left-hand panel). The results indicated that Rfa2 undergoes cell-cycle-dependent phosphorylation. In HF (hyphal form) WT cells induced by serum at 37 °C, Rfa2 phosphorylation was observed after 120 min and started to diminish at 240 min after hyphal induction (Figure 2A, top right-hand panel). In sharp contrast, Rfa2 was persistently phosphorylated in *pph3Δ* mutant cells under both yeast and hyphal growth conditions (Figure 2A, bottom panels).

We next tested the effect of the DNA replication inhibitor HU on Rfa phosphorylation. We observed that growing WT yeast cells in the presence of HU resulted in Rfa2 hyperphosphorylation, and subsequent shifting of the cells to HU-free media caused its gradual dephosphorylation (Figure 2B). In contrast, while Rfa2 in *pph3Δ* and *psy3Δ* cells became hyperphosphorylated in response to HU treatment, the level of Rfa2 phosphorylation continued to increase after HU removal (Figure 2B).

Hence, we concluded that Pph3 is responsible for Rfa2 dephosphorylation both during the cell cycle and under HU treatment.

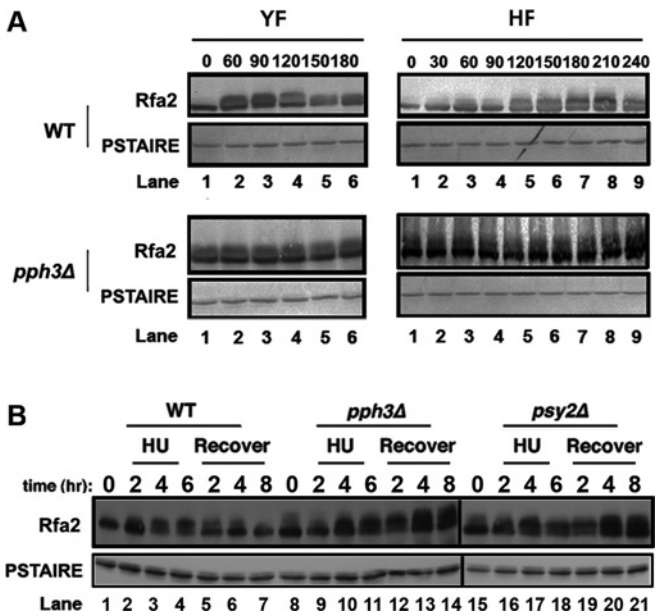

Figure 2 Pph3 is responsible for Rfa2 dephosphorylation during normal growth and under DNA replication stress

(**A**) WT (HT1) and *pph3Δ* (HT2) G_1 cells were released into conditions for yeast (YF) or hyphal (HF) growth. Aliquots of cells were harvested at the indicated times for Western blot analysis of Rfa2. (**B**) WT (HT1), *pph3Δ* (HT2) and *psy2Δ* (HT3) G_1 cells were first treated with 20 mM HU and then allowed to recover by transferring cells to HU-free medium for further growth. Aliquots of cells were harvested at the times indicated during both HU treatment and the recovery period for Western blot analysis of Rfa2.

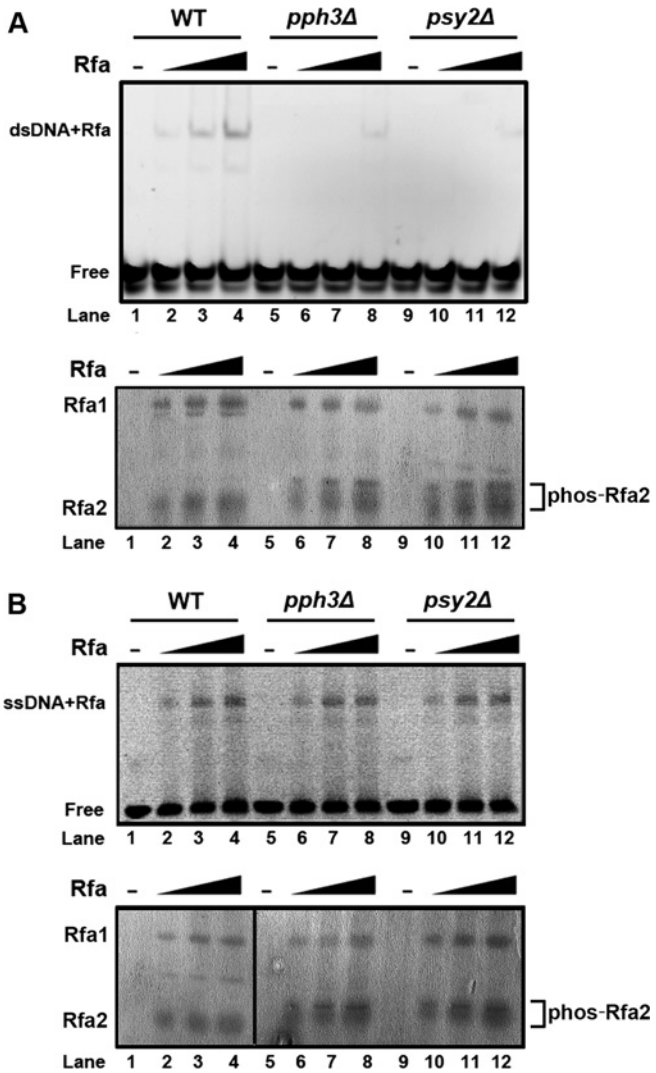

Figure 3 EMSA of Rfa2 with dsDNA and ssDNA

(**A**) Top panel: Rfa2 affinity-purified from WT (HT41), *pph3Δ* (HT42) and *psy2Δ* (HT43) cells was incubated with FITC-labelled dsDNA at molar ratios of DNA/protein of 0, 8, 16 and 32 at room temperature for 30 min. The protein/DNA mixture was then resolved by TGE/PAGE (8 % gel) and detected by fluorescence at an emission wavelength of 320 nm. Bottom panel: the same amounts of purified Rfa2 as above were resolved by SDS/PAGE (12 % gel) as a protein loading control. (**B**) The experiment described above was repeated using ssDNA instead of dsDNA.

Phosphorylated Rfa2 exhibited diminished binding activity to dsDNA, but not to ssDNA

Oakley et al. [31] showed previously that phosphorylated RPA2 extracted from mitotic human cells had little dsDNA-binding activity, whereas unphosphorylated recombinant RPA2 purified from bacteria exhibited dsDNA-binding activity. In the present study, we discovered that Rfa2 extracted from *pph3Δ* or *psy2Δ* cells also exhibited diminished binding to dsDNA compared with Rfa2 from WT cells in an EMSA (Figure 3A). Consistent with previous studies [31], ssDNA binding of Rfa2 purified from *pph3Δ* or *psy2Δ* cells was unaffected (Figure 3B). Therefore the results of the present study are consistent with the concept that phosphorylation of Rfa2 abolishes its binding to dsDNA, but not ssDNA [3,4,31].

Different domains of Rfa2 are (de)phosphorylated under different conditions in *C. albicans*

Thr^{43} in DBD-D is the only consensus CDK (cyclin-dependent kinase) phosphorylation site present on *C. albicans* Rfa2. Next, we tried to decipher the sites of phosphorylation on Rfa2 under normal growth conditions and DNA replication inhibition. We examined Rfa2 phosphorylation by Western blot analysis in different kinase-deficient *C. albicans* mutants. We first used a strain expressing the mutant Cdc28-as kinase which can be inhibited by the ATP analogue 1NM-PP1. We found that Rfa2 phosphorylation was not detectable in either YF or HF cells when 1NM-PP1 was added to the cultures. In comparison, Rfa2 phosphorylation was detected to be normal in the *mec1Δ/MET3-MEC1* (*MEC1* was shown to decrease by adding methionine and cysteine to the medium), *mrc1Δ*, *rad9Δ* and *ime2Δ* mutants grown under normal growth conditions (Figure 4A, left-hand panel). However, Rfa2 remained dephosphorylated only in the *mec1Δ/MET3-MEC1* mutant after HU treatment (Figure 4A, right-hand panel). Moreover, co-IP showed that Cdc28 directly interacted with Rfa2 in both yeast and hyphal cells under normal growth conditions (Figure 4C). However, in spite of repeated efforts, we failed to observe an interaction between Rfa2 and Mec1 in co-IP experiments (results not shown). We cannot rule out the possibility of transient or weak interaction between the proteins. Nevertheless, the results of the present study support a proposal that Cdc28 and Mec1 are responsible for Rfa2 phosphorylation during a normal cell cycle and under HU stress respectively.

Next, we wanted to determine whether the phosphorylation sites on Rfa2 that occurred during normal growth differ from those induced by HU treatment. First, we constructed two truncated forms of Rfa2: Rfa2-NΔ40 containing residues 41–272 and Rfa2-CΔ182 containing residues 1–190 (Figure 5A). We then expressed the two truncated versions of Rfa2 in WT and *pph3Δ* cells under

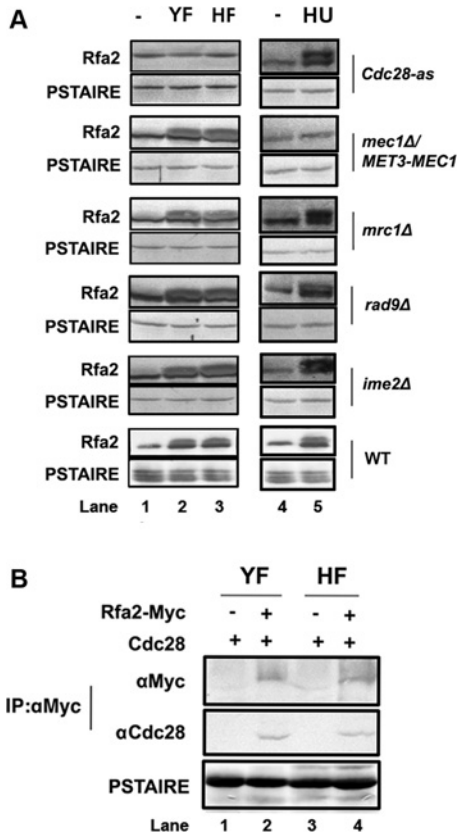

Figure 4 Role of Cdc28 and Mec1 in Rfa2 phosphorylation during normal growth and under HU treatment

(**A**) Western blot analysis of Rfa2 extracted from WT (HT1), *Cdc28-as* (HT40), *mec1Δ/MET3-MEC1* (HT37), *mrc1Δ* (HT34), *rad9Δ* (HT35) and *ime2Δ* (HT39) cells in G_1-phase, yeast growth (YF) and hyphal growth (HF) (left-hand panel) or after HU treatment for 4 h (right-hand panel). The anti-PSTAIRE antibody was used to show that equal amounts of protein were used. (**B**) Co-IP analysis of Cdc28 with Rfa2. Cells expressing Rfa2–Myc (HT1) were grown as yeast (YF) or hyphae (HF) for co-IP analysis. Rfa2 was pulled down with an anti-Myc antibody, followed by Western blot analysis with anti-Myc or anti-PSTAIRE antibodies.

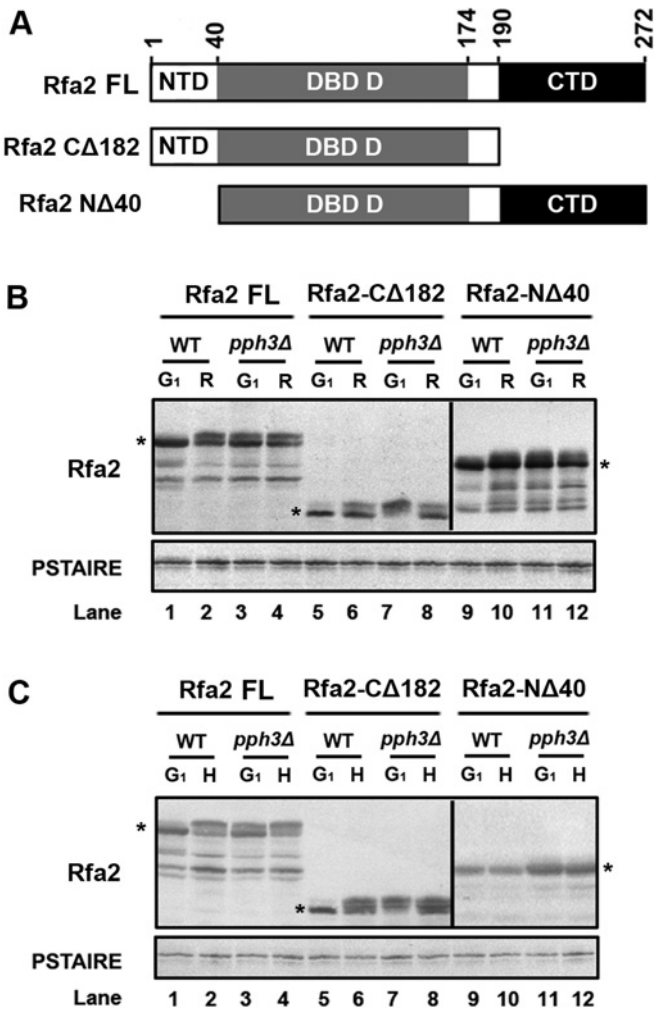

Figure 5 Different domains on Rfa2 are (de)phosphorylated under different circumstances

(**A**) Schematic description of FL and truncated versions of Rfa2. Rfa2-FL (HT1 and HT2), Rfa2-CΔ182 (HT31 and HT33) containing residues 1–190 and Rfa2-NΔ40 (HT30 and HT32) containing residues 41–272 were expressed in WT or *pph3Δ* (SJL2) mutant cells. (**B**) Western blot analysis of Rfa2 extracted from WT (HT1, HT30 and HT31) and *pph3Δ* (HT2, HT32 and HT33) cells expressing different versions of Rfa2 in G_1-phase and after release. An anti-PSTAIRE antibody was used to detect Cdc28 as a loading control. (**C**) Western blot analysis of Rfa2 extracted from the same set of cells as above during G_1-phase and after HU treatment.

normal growth conditions and HU treatment. The phosphorylation status of the two truncated Rfa2 proteins was examined by Western blot analysis in comparison with the FL (full-length) WT Rfa2 (Rfa2-FL). The results showed that in WT cells both truncated forms of Rfa2 were dephosphorylated during G_1-phase (Figure 5B, lanes 1, 5 and 9) and became phosphorylated 90 min after release (Figure 5B, lanes 2, 6 and 10). In contrast, Rfa2-FL, Rfa2-NΔ40 and Rfa2-CΔ182 expressed in the *pph3Δ* mutant cells were phosphorylated during G_1 arrest (Figure 5B, lanes 3, 7 and 11), and the phosphorylation persisted at 90 min (Figure 5B, lanes 4, 8 and 12). Therefore these results demonstrated that: (i) unlike the predominant phosphorylation of RPA2 in the NTD reported in previous studies [13,36,38–41], the NTD of Rfa2 is not the only domain phosphorylated during normal growth in *C. albicans*; and (ii) Pph3 is responsible for dephosphorylating Rfa2 during G_1-phase.

Next, Western blot analysis of HU-treated WT and *pph3Δ* cells expressing Rfa2-FL, Rfa2-NΔ40 and Rfa2-CΔ182 showed that Rfa2-FL and Rfa2-CΔ182, but not Rfa2-NΔ40, became phosphorylated in WT cells (Figure 5C, lanes 2, 6 and 8), whereas all three proteins were phosphorylated in *pph3Δ* cells (Figure 5C, lanes 4, 8 and 12). Therefore we observed that Rfa2-NΔ40 containing the DBD-D and CTDs existed in dephosphorylated form in WT, but not *pph3Δ*, cells after HU treatment in *C. albicans*. We deduced that the persistent phosphorylation of Rfa2-NΔ40 in *pph3Δ* cells before and after HU treatment (Figure 5C, lanes 11 and 12) might reflect the background level of phosphorylation as seen in normal cells (Figure 5B, lanes 11 and 12). Hence, this result suggests that the NTD is involved in response to DNA replication stress.

Next, we tried to map phosphorylation sites on Rfa2 extracted from *pph3Δ* mutant cells under normal growth conditions by MS. Results showed that the only consensus CDK phosphorylation site, Thr^{43}, was phosphorylated (Figure 6A). Additionally, Ser^{146} and Ser^{153} were two other phosphorylation sites with the highest probabilities (Figure 6A). Eight other potential phosphorylation sites, Thr^{24}, Thr^{34}/Thr^{35}/Thr^{36}, Ser^{148}, Ser^{211}, Thr^{213} and Ser^{247}, were also identified (Table 1). Sequence alignment of these potential phosphorylation sites of *C. albicans* Rfa2 with RPA2 in human, mouse, frog and zebrafish revealed little homology. However, Thr^{43} of *C. albicans* Rfa2 is conserved with Thr^{40} in *S. cerevisiae* Rfa2 (Figure 6B).

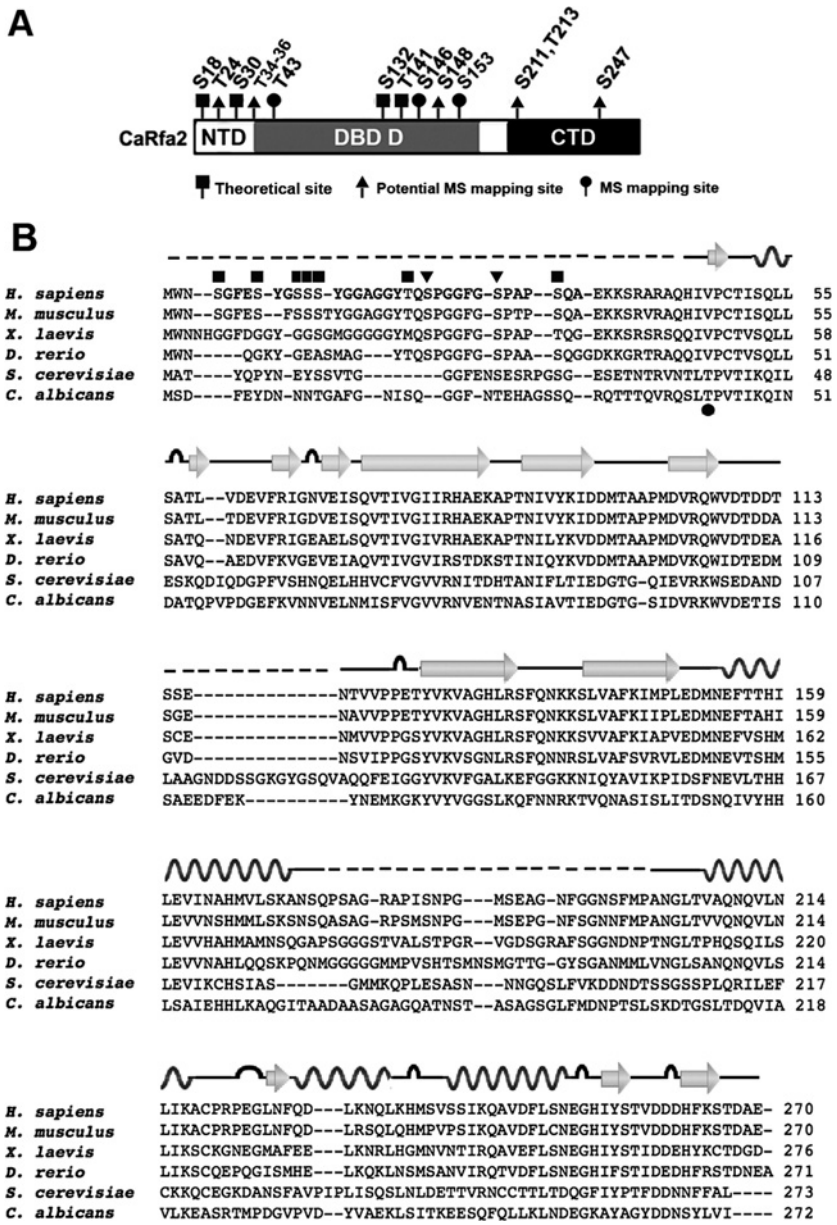

Figure 6 Potential dephosphoryation sites on Rfa2 mediated by Pph3 during normal growth

(**A**) Domain structure of Rfa2 depicting potential dephosphorylation sites mediated by Pph3. Rfa2 extracted from *pph3Δ* (HT2) cells was subject to MS analysis to map potential dephosphorylation sites mediated by Pph3 during normal growth phase. A black square denotes theoretical phosphorylation sites listed on the Uniprot database; a black triangle denotes phosphorylated sites mapped by MS with medium-high probability; and a black circle denotes phosphorylated sites mapped by MS with high probability. (**B**) Sequence alignment of Rfa2 and homologues in *Homo sapiens*, *Mus musculus*, *Xenopus laevis*, *Danio rerio*, *S. cerevisiae* and *C. albicans*. The secondary structure of human RPA2 (PDB codes 2PQA and 1Z1D) is illustrated above the sequence, where wave lines denotes α-helix, arrows denote β-strand, loops denote turns and broken lines denote unstructured regions. Black squares denote empirical DNA-PK and PI3K phosphorylation sites on human RPA2; black triangles denote CDK phosphorylation sites on human RPA2; and the black circle denotes the phospho-threonine mapped on *C. albicans* Rfa2 in the present study.

Finally, we performed alanine mutagenesis on the most probable phosphorylation sites occurring in different domains of Rfa2 identified by MS (Table 1) and investigated the phosphorylation state of these mutant proteins in G_1 cells and cells treated with HU. Western blot analysis showed that the Rfa2-T43A/S146A/S153A mutant remained unphosphorylated in G_1 cells (Figure 7A), but not in HU-treated cells (Figure 7B). This observation is consistent with our finding that domains other than the NTD is phosphorylated in G_1-phase (Figure 5B), and suggests that Thr^{43}, Ser^{146} and Ser^{153} in the DBD may play a critical role in a normal cell cycle. Ser^{18} and Ser^{30} in the NTD were predicted to be DNA-PK and PI3K (phosphoinositide 3-kinase) phosphorylation sites. We found that the Rfa2-S18A/S30A mutant showed significantly reduced phosphorylation on HU treatment (Figure 7B), confirming that the NTD, but not other domains, is essentially involved in Rfa2 phosphorylation under HU treatment (Figure 5C). The observation that the level of Rfa2-S18A/S30A phosphorylation was comparable with WT Rfa2 in G_1-phase (Figure 7A) further supports our finding that domains other than the NTD were phosphorylated during G_1-phase (Figure 5B). Furthermore, the Rfa2-S211A/T213A/S247A mutant showed a similar level of phosphorylation to WT Rfa2 both in G_1-phase (Figure 7A) and under HU treatment (Figure 7B), suggesting that the CTD plays a minor role in Rfa2 phosphoregulation.

Table 1 MS mapping of phosphorylation sites in Rfa2

Phosphorylation site mapping by tandem MS. Asterisks indicate phosphoserine or phosphothreonine residues. Consensus CDK phosphorylation sites are underlined.

Sequence of identified peptide	Position of phospho-residues
SQGGFNT*EHAGSSQRQ	Thr^{24}
RQT*T*TQVRQ	Thr^{34}, Thr^{35}
RQSLT*PVTIKQ	Thr^{43}
RQSLT*PVT*IKQ	Thr^{43}, Thr^{46}
RQS*LT*PVTIKQ	Ser^{41},Thr^{43}
TTQVRQSLT*PVTIKQ	Thr^{43}
RQTTT*QVRQSLT*PVTIKQ	Thr^{36}, Thr^{43}
RQTTT*QVRQSLT*PVT*IKQ	Thr^{36}, Thr^{43}, Thr^{46}
KTVQNASIS*LIT	Ser^{148}
RKTVQNASISLITDS*NQI	Ser^{153}
KT*VQNAS*ISLITDSNQIVYHHLSAIEHHLKA	Thr^{141}, Ser^{146}
KEES*QFQLLKL	Ser^{247}
RTMPDGVPVDYVAEKLSITKEES*QFQLLKL	Ser^{247}
KDTGS*LT*DQVIAVLKE	Ser^{211}, Thr^{213}
KAYAGYDDNS*YLVIEQKL	Ser^{268}
KYNEMKGKYVYVGGS*LKQFNNRK	Ser^{132}
KAQGITAADAASAGAGQATNSTAS*AGS* GLFMDNPT*S*LS*KD	Ser^{192}, Ser^{195}, Thr^{203}, Ser^{204}, Ser^{206}

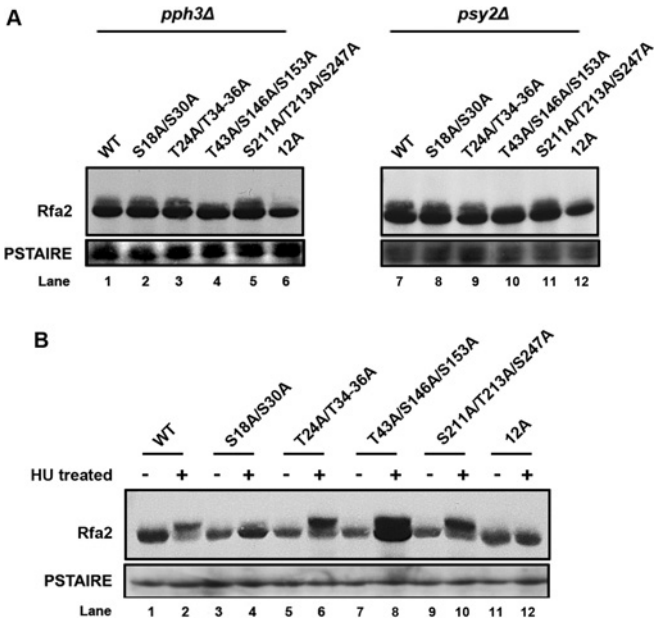

Figure 7 Identification of Rfa2 phosphorylation sites under different circumstances

(**A**) Western blot analysis of Rfa2 in *pph3*Δ (HT2, HT45, HT48, HT51, HT54 and HT57) and *psy2*Δ (HT3, HT46, HT49, HT52, HT55 and HT58) cells expressing different serine/threonine mutant alleles of *RFA2* in G_1 cells. An anti-PSTAIRE antibody was used to probe Cdc28 as a loading control. (**B**) Western blot analysis of Rfa2 in WT (HT1, HT44, HT47, HT50, HT53 and HT56) cells expressing different serine/threonine mutant alleles of *RFA2* before and after HU treatment.

Other mutants manifested similar phosphorylation patterns as WT Rfa2. It is to be noted that the mutant Rfa2 (Rfa2-12A) with all 12 selected sites of Ser^{18}, Ser^{30}, Thr^{24}, Thr^{34}, Thr^{35}, Thr^{36}, Thr^{43}, Ser^{146}, Ser^{153}, Ser^{211}, Thr^{213} and Ser^{247} mutated to alanine, remained unphosphorylated in G_1-phase in both *pph3Δ* and *psy2Δ* mutants (Figure 7A) and on HU treatment in WT cells (Figure 7B), indicating that these sites are determinant for Rfa2 phosphorylation collectively. Taken together, these results support the idea that domains of Rfa2 that are (de)phosphorylated during a normal cell cycle are different from those phosphorylated in response to DNA replication stress in *C. albicans*.

DISCUSSION

Pph3 dephosphorylates Rfa2 during G_1-phase and HU treatment

In the present study, we found that the Pph3–Psy2 complex is responsible for Rfa2 dephosphorylation during G_1-phase and on HU treatment. However, it was reported that PP4R2, but not PP4R3 (corresponding to Psy4 and Psy2 respectively in yeast) mediated RPA2 dephosphorylation in humans [44]. Although we could not rule out a role for Psy4 in Rfa2 dephosphorylation in *C. albicans*, the results of the present study clearly demonstrated that, distinct from humans, Psy2 is required for Rfa2 dephosphorylation. Further studies on other regulatory subunits of Pph3 need to be carried out to determine whether other Pph3 complexes have a role in the regulation of Rfa2 dephosphorylation.

We also showed that Rfa2 extracted from *pph3Δ* cells exhibited diminished binding to dsDNA, but not ssDNA, a result consistent with reports by Oakley et al. [31]. However, Patrick et al. [47] showed that phosphorylated RPA2 binds more weakly to short ssDNA (8–11 nt), but not long ssDNA. In the present study, the length of ssDNA used was 30 nt and, therefore, our EMSA result is not contradictory to previous observations.

Rfa2 regulation involves differential phosphorylation of different domains

Different kinases have been inferred in Rfa2 phosphorylation. For instance, in human cells, the CDK Cdc2 was shown to phosphorylate RPA2 during S-phase [29], and Mec1 was implicated in RPA2 hyperphosphorylation during HU treatment [48]. In *S. cerevisiae*, the meiosis-specific kinase Ime2 was found to be an Rfa2 kinase [49] which was shown to phosphorylate Ser^{27} of Rfa2 in a distinct manner from the mitotic Cln2–Cdk1 complex [50]. In addition to phosphorylation, previous studies have also shown that the phosphatase PP2A dephosphorylates Thr^{21} and Ser^{33} of RPA2 to trigger DNA-repair pathways in response to HU treatment in humans [43], and that PP4 was responsible for RPA2 dephosphorylation triggered by DNA DSBs induced by camptothecin [44]. Thus differential phosphorylation is prevalent in RPA2 under different conditions.

Human RPA2 is phosphorylated during mitosis [31,33]. Ser^{23} and Ser^{29} in human RPA2 are two consensus CDK phosphorylation sites (SP/TP) which are conserved from zebrafish to humans (Figure 6B, black triangle); however, these two SP/TP sites are not conserved in plants such as *Arabidopsis thaliana* or yeast such as *S. cerevisiae* or *C. albicans*. We noticed that Thr^{43} in *C. albicans* Rfa2 (corresponding to Thr^{40} in *S. cerevisiae*) is the sole predicted CDK site that aligns to a conserved valine–proline site in RPA2 of higher eukaryotes (Figure 6B, black circle). In the present study, MS indicated that Thr^{43} was phosphorylated in *pph3Δ* mutant cells, which replicated slightly faster than WT cells under unperturbed conditions (Supplementary Figure S2 at http://www.biochemj.org/bj/449/bj4490673add.htm), but lost viability more rapidly than WT cells in response to genotoxic stress [46]. In support of this observation, the Rfa2-T43A/S146A/S153A triple mutant remained unphosphorylated in

G_1-phase in both *pph3Δ* and *psy2Δ* cells (Figure 7A). Although the results of the present study suggest that mutating Thr^{43}, Ser^{146} and Ser^{153} is sufficient to block Rfa2 phosphorylation during G_1-phase, single-residue mutation is necessary to delineate the role of each residue. Nevertheless, the results of the present study support the notion that the DBD which harbours these residues is phosphorylated during G_1-phase (Figures 5B, 6A and 7A). Sequence identities of *C. albicans* Rfa2 to human, mouse, *Xenopus* and zebrafish RPA2 are 22.7, 23.1, 23.7 and 20.4 % respectively, compared with a slightly higher identity of 29.4 % to *S. cerevisiae* Rfa2, where homology mainly exists in their DBDs. In this context, it is hard to predict whether phosphorylation in regions other than the NTD of RPA2 occurs in other eukaryotes. Currently, reports on RPA2 are limited in other organisms. Hence, we do not know whether this phenomenon is unique in *C. albicans*.

Under certain stress conditions, many sites were shown to be phosphosphorylated in human RPA2 [13,35–41] (Figure 6B, black square), and the majority of these sites were found to be located in the NTD. Among these sites, Ser^{18} and Ser^{30} in *C. albicans* Rfa2 (corresponding to Thr^{21} and Ser^{33} in human RPA2) are conserved. The results of the present study show that, on HU treatment, Rfa2-FL and Rfa2-CΔ182 became phosphorylated, whereas Rfa2-NΔ40 remained dephosphorylated in WT cells, indicating possible phosphorylation in the NTD in *C. albicans* Rfa2 after HU treatment. Mutagenesis on Ser^{18} and Ser^{30} demonstrated that these sites partially contribute to Rfa2 phosphorylation during HU treatment (Figure 7B). Therefore we speculate that regulation of Rfa2 phosphorylation in *C. albicans* upon HU treatment also occurs in its NTD, similar to humans.

In summary, the present study has shown that: (i) the Pph3–Psy2 complex is responsible for Rfa2 dephosphorylation both during G_1-phase and under DNA replication stress in *C. albicans*; and (ii) different domains of Rfa2 are (de)phosphorylated under different circumstances.

AUTHOR CONTRIBUTION

Haitao Wang, Ada Wong, Jianli Sang and Yue Wang conceived and designed the experiments. Haitao Wang, Jiaxin Gao and Kangdi Hu performed the experiments. Haitao Wang, Ada Wong, Jianli Sang, Wanjie Li and Yue Wang analysed the data. Ada Wong, Yue Wang and Haitao Wang wrote the paper.

ACKNOWLEDGEMENTS

We thank members of the Sang laboratory for comments and suggestions on the paper before submission.

FUNDING

This work was supported by the National Basic Research Program of China [grant number 2007CB914401], the National Natural Science Foundation of China [grant number 31270113] and the Fundamental Research Funds for the Central Universities [grant number 105566GK].

REFERENCES

1 Brill, S. J. and Stillman, B. (1991) Replication factor-A from *Saccharomyces cerevisiae* is encoded by three essential genes coordinately expressed at S phase. Genes Dev. **5**, 1589–1600
2 Santocanale, C., Neecke, H., Longhese, M. P., Lucchini, G. and Plevani, P. (1995) Mutations in the gene encoding the 34 kDa subunit of yeast replication protein A cause defective S phase progression. J. Mol. Biol. **254**, 595–607
3 Fanning, E., Klimovich, V. and Nager, A. R. (2006) A dynamic model for replication protein A (RPA) function in DNA processing pathways. Nucleic Acids Res. **34**, 4126–4137
4 Broderick, S., Rehmet, K., Concannon, C. and Nasheuer, H. P. (2010) Eukaryotic single-stranded DNA binding proteins: central factors in genome stability. Subcell. Biochem. **50**, 143–163
5 Binz, S. K., Lao, Y., Lowry, D. F. and Wold, M. S. (2003) The phosphorylation domain of the 32-kDa subunit of replication protein A (RPA) modulates RPA–DNA interactions. Evidence for an intersubunit interaction. J. Biol. Chem. **278**, 35584–35591
6 Henricksen, L. A., Umbricht, C. B. and Wold, M. S. (1994) Recombinant replication protein A: expression, complex formation, and functional characterization. J. Biol. Chem. **269**, 11121–11132
7 He, Z., Henricksen, L. A., Wold, M. S. and Ingles, C. J. (1995) RPA involvement in the damage-recognition and incision steps of nucleotide excision repair. Nature **374**, 566–569
8 Weisshart, K., Pestryakov, P., Smith, R. W., Hartmann, H., Kremmer, E., Lavrik, O. and Nasheuer, H. P. (2004) Coordinated regulation of replication protein A activities by its subunits p14 and p32. J. Biol. Chem. **279**, 35368–35376
9 Sugiyama, T. and Kowalczykowski, S. C. (2002) Rad52 protein associates with replication protein A (RPA)-single-stranded DNA to accelerate Rad51-mediated displacement of RPA and presynaptic complex formation. J. Biol. Chem. **277**, 31663–31672
10 Gomes, X. V. and Wold, M. S. (1995) Structural analysis of human replication protein A. Mapping functional domains of the 70-kDa subunit. J. Biol. Chem. **270**, 4534–4543
11 Wold, M. S. (1997) Replication protein A: a heterotrimeric, single-stranded DNA-binding protein required for eukaryotic DNA metabolism. Annu. Rev. Biochem. **66**, 61–92
12 Oakley, G. G., Loberg, L. I., Yao, J., Risinger, M. A., Yunker, R. L., Zernik-Kobak, M., Khanna, K. K., Lavin, M. F., Carty, M. P. and Dixon, K. (2001) UV-induced hyperphosphorylation of replication protein a depends on DNA replication and expression of ATM protein. Mol. Biol. Cell **12**, 1199–1213
13 Nuss, J. E., Patrick, S. M., Oakley, G. G., Alter, G. M., Robison, J. G., Dixon, K. and Turchi, J. J. (2005) DNA damage induced hyperphosphorylation of replication protein A. 1. Identification of novel sites of phosphorylation in response to DNA damage. Biochemistry **44**, 8428–8437
14 Mer, G., Bochkarev, A., Gupta, R., Bochkareva, E., Frappier, L., Ingles, C. J., Edwards, A. M. and Chazin, W. J. (2000) Structural basis for the recognition of DNA repair proteins UNG2, XPA, and RAD52 by replication factor RPA. Cell **103**, 449–456
15 Arunkumar, A. I., Klimovich, V., Jiang, X., Ott, R. D., Mizoue, L., Fanning, E. and Chazin, W. J. (2005) Insights into hRPA32 C-terminal domain-mediated assembly of the simian virus 40 replisome. Nat. Struct. Mol. Biol. **12**, 332–339
16 de Laat, W. L., Appeldoorn, E., Sugasawa, K., Weterings, E., Jaspers, N. G. and Hoeijmakers, J. H. (1998) DNA-binding polarity of human replication protein A positions nucleases in nucleotide excision repair. Genes Dev. **12**, 2598–2609
17 Bochkareva, E., Korolev, S., Lees-Miller, S. P. and Bochkarev, A. (2002) Structure of the RPA trimerization core and its role in the multistep DNA-binding mechanism of RPA. EMBO J. **21**, 1855–1863
18 Bochkareva, E., Belegu, V., Korolev, S. and Bochkarev, A. (2001) Structure of the major single-stranded DNA-binding domain of replication protein A suggests a dynamic mechanism for DNA binding. EMBO J. **20**, 612–618
19 Bastin-Shanower, S. A. and Brill, S. J. (2001) Functional analysis of the four DNA binding domains of replication protein A. The role of RPA2 in ssDNA binding. J. Biol. Chem. **276**, 36446–36453
20 Wyka, I. M., Dhar, K., Binz, S. K. and Wold, M. S. (2003) Replication protein A interactions with DNA: differential binding of the core domains and analysis of the DNA interaction surface. Biochemistry **42**, 12909–12918
21 Arunkumar, A. I., Stauffer, M. E., Bochkareva, E., Bochkarev, A. and Chazin, W. J. (2003) Independent and coordinated functions of replication protein A tandem high affinity single-stranded DNA binding domains. J. Biol. Chem. **278**, 41077–41082
22 Blackwell, L. J., Borowiec, J. A. and Mastrangelo, I. A. (1996) Single-stranded-DNA binding alters human replication protein A structure and facilitates interaction with DNA-dependent protein kinase. Mol. Cell. Biol. **16**, 4798–4807
23 Bochkarev, A., Pfuetzner, R. A., Edwards, A. M. and Frappier, L. (1997) Structure of the single-stranded-DNA-binding domain of replication protein A bound to DNA. Nature **385**, 176–181
24 Pestryakov, P. E., Khlimankov, D. Y., Bochkareva, E., Bochkarev, A. and Lavrik, O. I. (2004) Human replication protein A (RPA) binds a primer-template junction in the absence of its major ssDNA-binding domains. Nucleic Acids Res. **32**, 1894–1903
25 Pestryakov, P. E., Weisshart, K., Schlott, B., Khodyreva, S. N., Kremmer, E., Grosse, F., Lavrik, O. I. and Nasheuer, H. P. (2003) Human replication protein A. The C-terminal RPA70 and the central RPA32 domains are involved in the interactions with the 3′-end of a primer-template DNA. J. Biol. Chem. **278**, 17515–17524
26 Dickson, A. M., Krasikova, Y., Pestryakov, P., Lavrik, O. and Wold, M. S. (2009) Essential functions of the 32 kDa subunit of yeast replication protein A. Nucleic Acids Res. **37**, 2313–2326
27 Henricksen, L. A. and Wold, M. S. (1994) Replication protein A mutants lacking phosphorylation sites for p34cdc2 kinase support DNA replication. J. Biol. Chem. **269**, 24203–24208

28 Dutta, A. and Stillman, B. (1992) cdc2 family kinases phosphorylate a human cell DNA replication factor, RPA, and activate DNA replication. EMBO J. **11**, 2189–2199
29 Fang, F. and Newport, J. W. (1993) Distinct roles of cdk2 and cdc2 in RP-A phosphorylation during the cell cycle. J. Cell Sci. **106**, 983–994
30 Stephan, H., Concannon, C., Kremmer, E., Carty, M. P. and Nasheuer, H. P. (2009) Ionizing radiation-dependent and independent phosphorylation of the 32-kDa subunit of replication protein A during mitosis. Nucleic Acids Res. **37**, 6028–6041
31 Oakley, G. G., Patrick, S. M., Yao, J., Carty, M. P., Turchi, J. J. and Dixon, K. (2003) RPA phosphorylation in mitosis alters DNA binding and protein–protein interactions. Biochemistry **42**, 3255–3264
32 Binz, S. K. and Wold, M. S. (2008) Regulatory functions of the N-terminal domain of the 70-kDa subunit of replication protein A (RPA). J. Biol. Chem. **283**, 21559–21570
33 Anantha, R. W., Sokolova, E. and Borowiec, J. A. (2008) RPA phosphorylation facilitates mitotic exit in response to mitotic DNA damage. Proc. Natl. Acad. Sci. U.S.A. **105**, 12903–12908
34 Anantha, R. W. and Borowiec, J. A. (2009) Mitotic crisis: the unmasking of a novel role for RPA. Cell Cycle **8**, 357–361
35 Liaw, H., Lee, D. and Myung, K. (2011) DNA-PK-dependent RPA2 hyperphosphorylation facilitates DNA repair and suppresses sister chromatid exchange. PLoS ONE **6**, e21424
36 Zernik-Kobak, M., Vasunia, K., Connelly, M., Anderson, C. W. and Dixon, K. (1997) Sites of UV-induced phosphorylation of the p34 subunit of replication protein A from HeLa cells. J. Biol. Chem. **272**, 23896–23904
37 Niu, H., Erdjument-Bromage, H., Pan, Z. Q., Lee, S. H., Tempst, P. and Hurwitz, J. (1997) Mapping of amino acid residues in the p34 subunit of human single-stranded DNA-binding protein phosphorylated by DNA-dependent protein kinase and Cdc2 kinase *in vitro*. J. Biol. Chem. **272**, 12634–12641
38 Carty, M. P., Zernik-Kobak, M., McGrath, S. and Dixon, K. (1994) UV light-induced DNA synthesis arrest in HeLa cells is associated with changes in phosphorylation of human single-stranded DNA-binding protein. EMBO J. **13**, 2114–2123
39 Olson, E., Nievera, C. J., Klimovich, V., Fanning, E. and Wu, X. (2006) RPA2 is a direct downstream target for ATR to regulate the S-phase checkpoint. J. Biol. Chem. **281**, 39517–39533
40 Shao, R. G., Cao, C. X., Zhang, H., Kohn, K. W., Wold, M. S. and Pommier, Y. (1999) Replication-mediated DNA damage by camptothecin induces phosphorylation of RPA by DNA-dependent protein kinase and dissociates RPA:DNA-PK complexes. EMBO J. **18**, 1397–1406
41 Morgan, S. E. and Kastan, M. B. (1997) Dissociation of radiation-induced phosphorylation of replication protein A from the S-phase checkpoint. Cancer Res. **57**, 3386–3389
42 Vassin, V. M., Wold, M. S. and Borowiec, J. A. (2004) Replication protein A (RPA) phosphorylation prevents RPA association with replication centers. Mol. Cell. Biol. **24**, 1930–1943
43 Feng, J., Wakeman, T., Yong, S., Wu, X., Kornbluth, S. and Wang, X. F. (2009) Protein phosphatase 2A-dependent dephosphorylation of replication protein A is required for the repair of DNA breaks induced by replication stress. Mol. Cell. Biol. **29**, 5696–5709
44 Lee, D. H., Pan, Y., Kanner, S., Sung, P., Borowiec, J. A. and Chowdhury, D. (2010) A PP4 phosphatase complex dephosphorylates RPA2 to facilitate DNA repair via homologous recombination. Nat. Struct. Mol. Biol. **17**, 365–372
45 Shi, Q. M., Wang, Y. M., Zheng, X. D., Lee, R. T. and Wang, Y. (2007) Critical role of DNA checkpoints in mediating genotoxic-stress-induced filamentous growth in *Candida albicans*. Mol. Biol. Cell **18**, 815–826
46 Wang, H., Gao, J., Li, W., Wong, A. H., Hu, K., Chen, K., Wang, Y. and Sang, J. (2012) Pph3 dephosphorylation of Rad53 is required for cell recovery from MMS-induced DNA damage in *Candida albicans*. PLoS ONE **7**, e37246
47 Patrick, S. M., Oakley, G. G., Dixon, K. and Turchi, J. J. (2005) DNA damage induced hyperphosphorylation of replication protein A.2. Characterization of DNA binding activity, protein interactions, and activity in DNA replication and repair. Biochemistry **44**, 8438–8448
48 Brush, G. S., Morrow, D. M., Hieter, P. and Kelly, T. J. (1996) The ATM homologue MEC1 is required for phosphorylation of replication protein A in yeast. Proc. Natl. Acad. Sci. U.S.A. **93**, 15075–15080
49 Clifford, D. M., Marinco, S. M. and Brush, G. S. (2004) The meiosis-specific protein kinase Ime2 directs phosphorylation of replication protein A. J. Biol. Chem. **279**, 6163–6170
50 Sawarynski, K. E., Kaplun, A., Tzivion, G. and Brush, G. S. (2007) Distinct activities of the related protein kinases Cdk1 and Ime2. Biochim. Biophys. Acta **1773**, 450–456

Received 9 June 2012/7 November 2012; accepted 9 November 2012
Published as BJ Immediate Publication 9 November 2012, doi:10.1042/BJ20120952

Biochem. J. (2013) **449**, 673–681 (Printed in Great Britain) doi:10.1042/BJ20120952

online data

SUPPLEMENTARY ONLINE DATA
Rfa2 is specifically dephosphorylated by Pph3 in *Candida albicans*

Haitao WANG*†[1], Jiaxin GAO*[1], Ada Hang-Heng WONG‡, Kangdi HU*, Wanjie LI*, Yue WANG†[2] and Jianli SANG*[2]

*Key Laboratory of Cell Proliferation and Regulation Biology, Ministry of Education, College of Life Sciences, Beijing Normal University, Beijing 100875, People's Republic of China, †Institute of Molecular and Cell Biology, Agency for Science, Technology and Research (A*STAR), Singapore 138673, and ‡Protein Science Laboratory, School of Life Sciences, Tsinghua University, Beijing 100084, People's Republic of China

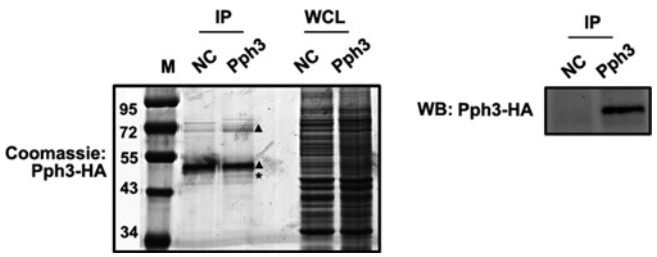

Figure S1 SDS/PAGE of immunopurified Pph3 from WT *C. albicans* cells

Left-hand side: C-terminally HA (haemagglutinin)-tagged Pph3 was immunopurified by an anti-HA antibody from *C. albicans* cells (HT28 and HT29) and resolved by SDS/PAGE (10% gel). The asterisk denotes Pph3 and triangles denote the antibody fragments. Right-hand side: Western blotting of the immunopurified Pph3 using an anti-HA antibody.

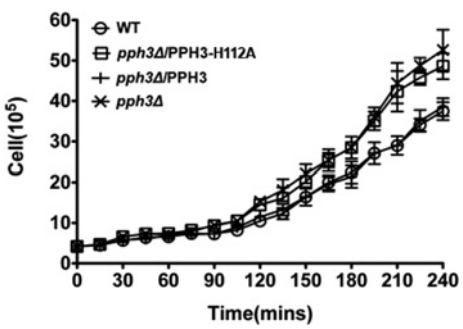

Figure S2 Cell growth in wild-type, *pph3Δ/PPH3-H112A*, *pph3Δ/PPH3* and *pph3Δ* mutant cells

WT (SC5314 or BWP17), *pph3Δ/PPH3-H112A* (HT29), *pph3Δ/PPH3* (HT28) and *pph3Δ* (SJL3) mutant cells were grown in liquid YPD medium at 30°C for 4 h. Cells were counted in triplicate parallel experiments at the times indicated.

[1] These authors contributed equally to this work.
[2] Correspondence may be addressed to either of these authors (email jlsang@bnu.edu.cn or mcbwangy@imcb.a-star.edu.sg).

Table S1 ***C. albicans*** **strains used in the present study**

Strains	Relevant genotype	Source
SC5314	WT, clinical isolate	
BWP17	ura3 /ura3 his1::hisG/his1::hisG arg4::hisG/arg4::hisG	[1]
SJL2	BWP17 pph3Δ::ARG4/ pph3Δ::HIS1	[2]
SJL2.1	BWP17 pph3Δ::ARG4/ pph3Δ::HIS1 PPH3:URA3	[2]
SJL3	BWP17 pph3Δ::ARG4/ pph3Δ::HIS1 URA3	[2]
SJL5	BWP17 psy2Δ::ARG4/ psy2Δ::HIS1	[2]
SJL5.1	BWP17 psy2Δ::ARG4/ psy2Δ::HIS1 PSY2:URA3	[2]
SJL6	BWP17 psy2Δ::ARG4/ psy2Δ::HIS1 URA3	[2]
HKD1.1	BWP17 ptc2Δ::ARG4/ ptc2Δ::HIS1 URA3	The present study
HKD2	BWP17 pph3Δ::ARG4/ pph3Δ::HIS1 ptc2Δ::FRT/ ptc2Δ::FRT URA3	The present study
HT1	BWP17 RFA2-Myc::URA3	[2]
HT2	BWP17 pph3Δ::ARG4/ pph3Δ::HIS1 RFA2-Myc:URA3	[2]
HT3	BWP17 psy2Δ::ARG4/ psy2Δ::HIS1 RFA2-Myc:URA3	[2]
HT4	BWP17 ptc2Δ::ARG4/ ptc2Δ::HIS1 RFA2-Myc:URA3	[2]
HT5	BWP17 pph3Δ::ARG4/pph3Δ::HIS1 ptc2Δ::FRT/ ptc2Δ::FRT RFA2-Myc:URA3	[2]
HT25	BWP17 glc7Δ::ARG4/PMET3-GLC7::HIS1 RFA2-Myc:URA3	The present study
HT26	BWP17 PPH3/PPH3-6MYC:URA3 RFA2/RFA2-GFP:HIS	The present study
HT27	BWP17 PSY2/PSY2-6MYC:URA3 RFA2/RFA2-GFP:HIS	The present study
HT28	BWP17 pph3Δ::ARG4/ pph3Δ::HIS1 PPH3-HA:URA3	The present study
HT29	BWP17 pph3Δ::ARG4/ pph3Δ::HIS1 pph3H112A-HA:URA3	The present study
HT30	BWP17 PMET3-MYC-Δ40-RFA2::URA3	The present study
HT31	BWP17 RFA2-190-MYC::URA3	The present study
HT32	BWP17 pph3Δ::ARG4/pph3Δ::HIS1 PMET3-MYC-Δ40-RFA2::URA3	The present study
HT33	BWP17 pph3Δ::ARG4/pph3Δ::HIS1 RFA2-190-MYC::URA3	The present study
WYS2	mrc1Δ::ARG4/mrc1Δ::HIS1	[3]
HT34	mrc1Δ::ARG4/mrc1Δ::HIS1 RFA2-Myc URA3	The present study
WYS1	rad9Δ::ARG4/rad9Δ::URA3	[3]
HT35	rad9Δ::ARG4/rad9Δ::URA3 RFA2-Myc HIS1	The present study
HT36	BWP17 mec1Δ::ARG4/PMET3-MEC1::URA3	The present study
HT37	BWP17 mec1Δ::ARG4/PMET3-MEC1::URA3 RFA2-Myc:HIS	The present study
HT38	BWP17 Ime2Δ::ARG4/ime2Δ::HIS1	The present study
HT39	BWP17 Ime2Δ::ARG4/ime2Δ::HIS1 RFA2-Myc:URA3	The present study
WY	BWP17 cdc28Δ::ARG4/PMET3-CDC28as::URA3	[3]
HT40	BWP17 cdc28Δ::ARG4/PMET3-CDC28as::URA3 RFA2-Myc:HIS1	The present study
HT41	BWP17 RFA2-HIS-tag-URA3	The present study
HT42	BWP17 pph3Δ::ARG4/ pph3Δ::HIS1 RFA2-HIS-tag:URA3	The present study
HT43	BWP17 psy2Δ::ARG4/ psy2Δ::HIS1 RFA2-HIS-tag:URA3	The present study
HT44	BWP17 rfa2S18A/S30A-Myc::URA3	The present study
HT45	BWP17 pph3Δ::ARG4/ pph3Δ::HIS1 rfa2S18A/S30A-Myc::URA3	The present study
HT46	BWP17 psy2Δ::ARG4/ psy2Δ::HIS1 rfa2S18A/S30A-Myc::URA3	The present study
HT47	BWP17 rfa2T24A/T34A/T35A/T36A-Myc::URA3	The present study
HT48	BWP17 pph3Δ::ARG4/ pph3Δ::HIS1 rfa2T24A/T34A/T35A/T36A-Myc::URA3	The present study
HT49	BWP17 psy2Δ::ARG4/ psy2Δ::HIS1 rfa2T24A/T34A/T35A/T36A-Myc::URA3	The present study
HT50	BWP17 rfa2T43A/S146A/S153A-Myc::URA3	The present study
HT51	BWP17 rfa2T43A/S146A/S153A-Myc::URA3	The present study
HT52	BWP17 rfa2T43A/S146A/S153A-Myc::URA3	The present study
HT53	BWP17 rfa2S211A/T213A/S247A-Myc::URA3	The present study
HT54	BWP17 pph3Δ::ARG4/ pph3Δ::HIS1 rfa2S211A/T213A/S247A-Myc::URA3	The present study
HT55	BWP17 psy2Δ::ARG4/ psy2Δ::HIS1 rfa2S211A/T213A/S247A-Myc::URA3	The present study
HT56	BWP17 rfa2S18A/T24A/T34A/T35A/T36A/T43A/S146A/S153A/S211A/T213A/S247A-Myc::URA3	The present study
HT57	BWP17 pph3Δ::ARG4/pph3Δ::HIS1 rfa2S18A/T24A/T34A/T35A/T36A/T43A/S146A/S153A/S211A/T213A/S247A-Myc::URA3	The present study
HT58	BWP17 psy2Δ::ARG4/psy2Δ::HIS1 rfa2S18A/T24A/T34A/T35A/T36A/T43A/S146A/S153A/S211A/T213A/S247A-Myc::URA3	The present study

REFERENCES

1 Wilson, R. B., Davis, D. and Mitchell, A. P. (1999) Rapid hypothesis testing with *Candida albicans* through gene disruption with short homology regions. J. Bacteriol. **181**, 1868–1874

2 Wang, H., Gao, J., Li, W., Wong, A. H., Hu, K., Chen, K., Wang, Y. and Sang, J. (2012) Pph3 dephosphorylation of Rad53 is required for cell recovery from MMS-induced DNA damage in *Candida albicans*. PLoS ONE **7**, e37246

3 Shi, Q. M., Wang, Y. M., Zheng, X. D., Lee, R. T. and Wang, Y. (2007) Critical role of DNA checkpoints in mediating genotoxic-stress-induced filamentous growth in *Candida albicans*. Mol. Biol. Cell **18**, 815–826

Received 9 June 2012/7 November 2012; accepted 9 November 2012
Published as BJ Immediate Publication 9 November 2012, doi:10.1042/BJ20120952